

行政院國家科學委員會補助專題研究計畫 成果報告
 期中進度報告

蒸氣流場下多層熱管之熱彈問題

計畫類別： 個別型計畫 整合型計畫

計畫編號：NSC-92-2212-E-164-005

執行期間： 92年8月1日至93年7月31日

計畫主持人：李宗乙

共同主持人：

計畫參與人員：林俊宏

成果報告類型(依經費核定清單規定繳交)： 精簡報告 完整報告

本成果報告包括以下應繳交之附件：

- 赴國外出差或研習心得報告一份
- 赴大陸地區出差或研習心得報告一份
- 出席國際學術會議心得報告及發表之論文各一份
- 國際合作研究計畫國外研究報告書一份

執行單位：修平技術學院

中 華 民 國 九 十 三 年 七 月 三 十 一 日

蒸氣流場下多層熱管之熱彈問題

計畫編號：NSC 92-2212-E-164-005

執行期限：92 年 8 月 1 日至 93 年 7 月 31 日

主持人：李宗乙 修平技術學院機械系

計畫參與人員：林俊宏 中興大學應用數學系研究生

摘要

本文主要是分析一異向性材料所組成的三維熱管在受熱與壓力耦合變化下，因壁內外邊界條件的差異而所產生的熱變形問題。而我們探討可分為內邊界和外邊界這二個部分，我們在內邊界部分管內開始加熱時利用熱力學蒸汽表模擬出蒸氣溫度和壓力的關係式當成邊界條件，溫度和壓力相互影響且隨時間變化下其暫態熱應力的分佈情形。而在外邊界部分我們假設為不同狀態而我們將使用有限差分法與拉氏轉換來處理此類問題。

關鍵字：熱管、熱變形、拉氏轉換

Abstract

This paper deals three-dimensional axisymmetric quasistatic-coupled thermo-elastic problems for time-dependent boundary condition. The water vapor temperature and pressure relation assumed for the inner boundary. The water vapor temperature and pressure data were obtained from a thermodynamic steam table. Laplace transform and finite difference methods are used to analyze problems. The solution is obtained by using the matrix similarity transformation and inverse Laplace transform. We obtain solutions for the temperature and thermal deformation distributions in a transient and steady state.

Keywords: Multilayered、Laplace transform

1. Introduction

Stasynk et al. [1] have studied the steady-state thermal stress of hollow cylinders considering the effect of variation of thermal conductivity as a function of temperature. They concluded that the effect of thermal conductivity on the temperature and stresses is slight for small values of internal heat flow. However, for large heat flow, the difference in temperature and stresses between temperature-dependent and independent thermal conductivity can be as much as 20%. Vollbrecht [2] has analyzed the stresses in both cylindrical and spherical walls subjected to internal pressure and stationary heat flow. Kandil [3] has studied the effect of steady-state temperature and pressure gradient on compound cylinders fitted together by shrink fit. The finite element method has been used by Sinha [4] to analyze the thermal stresses and temperature distribution in a hollow thick cylinder subjected to a steady-state heat load in the radial direction. Naga [5] has presented the stress analysis and the optimization of both thick-walled impermeable and permeable cylinders under the combined effect of steady-state temperature and pressure gradient.

2. Formulation

We now consider a finitely long annular cylinder made of different length as shown in Figure 1. The inner and outer radii of the

cylinder are denoted by r_i and r_0 respectively. The hollow cylinder is assumed to be heated suddenly at the inner and outer surface under temperatures f_1 and f_2 respectively.

The transient heat conduction equation for the axisymmetric cylinder is

$$[k_r \frac{\partial^2}{\partial r^{*2}} + k_\theta \frac{1}{r^*} \frac{\partial}{\partial r^*} + k_z \frac{\partial^2}{\partial z^{*2}}] \bar{\Theta} = \rho C_v \frac{\partial \bar{\Theta}}{\partial \tau} + \Theta_0 \beta_r \frac{\partial}{\partial r^*} \left(\frac{\partial U_r}{\partial \tau} \right) + \Theta_0 \beta_\theta \frac{1}{r^*} \left(\frac{\partial U_r}{\partial \tau} \right) + \Theta_0 \beta_z \frac{\partial}{\partial z^*} \left(\frac{\partial U_z}{\partial \tau} \right) \quad (1)$$

If the body forces are absent, the equation of equilibrium for a cylinder along the radial direction can be written as

$$\begin{aligned} & \frac{E_r(1-v_{\theta z}v_{z\theta})}{A} \frac{\partial^2 U_r}{\partial r^{*2}} + \frac{E_r(1-v_{\theta z}v_{z\theta})}{A} \frac{1}{r^*} \frac{\partial U_r}{\partial r^*} - \frac{E_\theta(1-v_{\theta z}v_{z\theta})}{A} \frac{1}{r^{*2}} U_r \\ & + G_{rz} \frac{\partial^2 U_r}{\partial z^{*2}} + [G_{rz} + \frac{E_z(v_{rz}+v_{r\theta}v_{\theta z})}{A}] \frac{\partial^2 U_z}{\partial r^* \partial z^*} \\ & - \frac{1}{A} [E_r(1-v_{\theta z}v_{z\theta})\alpha_r + E_\theta(v_{r\theta}+v_{z\theta}v_{rz})\alpha_\theta + E_z(v_{rz}+v_{r\theta}v_{\theta z})\alpha_z] \frac{\partial \bar{\Theta}}{\partial r^*} \\ & - \frac{1}{A} [E_r(1-v_{\theta z}v_{z\theta}) - E_\theta(v_{r\theta}+v_{z\theta}v_{rz})]\alpha_r + [E_\theta(v_{r\theta}+v_{z\theta}v_{rz}) \\ & - E_\theta(1-v_{\theta z}v_{z\theta})]\alpha_\theta + \frac{1}{r^*} \bar{\Theta} = 0 \end{aligned} \quad (2)$$

If the body forces are absent, the equation of equilibrium for a cylinder along the z-direction can be written as

$$\begin{aligned} & G_{rz} \frac{\partial^2 U_z}{\partial r^{*2}} + [G_{rz} + \frac{E_\theta(v_{rz}+v_{r\theta}v_{\theta z})}{A}] \frac{\partial^2 U_z}{\partial r^* \partial z^*} + \frac{G_{rz}}{r^*} \frac{\partial U_z}{\partial r^*} + \frac{E_z(1-v_{\theta z}v_{z\theta})}{A} \frac{\partial^2 U_z}{\partial z^{*2}} \\ & + [G_{rz} + \frac{E_z(v_{\theta z}+v_{\theta r}v_{rz})}{A}] \frac{1}{r^*} \frac{\partial U_r}{\partial z^*} \\ & - \frac{1}{A} [E_z(1-v_{\theta z}v_{z\theta})\alpha_z + E_z(v_{\theta z}+v_{\theta r}v_{rz})\alpha_\theta + E_\theta(v_{rz}+v_{r\theta}v_{\theta z})\alpha_r] \frac{\partial \bar{\Theta}}{\partial z^*} = 0 \end{aligned} \quad (3)$$

The stress-displacement relations are

$$\begin{aligned} \sigma_{r_i}^* &= \frac{1}{A} [E_r(1-v_{\theta z}v_{z\theta}) \frac{\partial U_r}{\partial r^*} + E_\theta(v_{r\theta}+v_{z\theta}v_{rz}) \frac{U_r}{r^*} + \\ & E_z(v_{rz}+v_{r\theta}v_{\theta z}) \frac{\partial U_z}{\partial z^*} - \beta_r(\Theta - \Theta_0)] \end{aligned} \quad (4)$$

$$\begin{aligned} \sigma_{\theta_i}^* &= \frac{1}{A} [E_\theta(v_{r\theta}+v_{z\theta}v_{rz}) \frac{\partial U_r}{\partial r^*} + E_\theta(1-v_{\theta z}v_{z\theta}) \frac{U_r}{r^*} + \\ & E_z(v_{rz}+v_{r\theta}v_{\theta z}) \frac{\partial U_z}{\partial z^*} - \beta_\theta(\Theta - \Theta_0)] \end{aligned} \quad (5)$$

$$\begin{aligned} \sigma_{z_i}^* &= \frac{1}{A} [E_\theta(v_{rz}+v_{r\theta}v_{\theta z}) \frac{\partial U_r}{\partial r^*} + E_z(v_{\theta z}+v_{\theta r}v_{rz}) \frac{U_r}{r^*} + \\ & E_z(1-v_{\theta z}v_{z\theta}) \frac{\partial U_z}{\partial z^*} - \beta_z(\Theta - \Theta_0)] \end{aligned} \quad (6)$$

$$\tau_{r_z}^* = G_{rz} \left(\frac{\partial U_z}{\partial r^*} + \frac{\partial U_r}{\partial z^*} \right) \quad (7)$$

where

$$A = 1 - v_{r\theta}v_{\theta r} - v_{\theta z}v_{z\theta} - v_{rz}v_{rz} - 2v_{\theta z}v_{z\theta}v_{rz}$$

$$\beta_r = \frac{1}{A} [E_r(1-v_{\theta z}v_{z\theta})\alpha_r + E_\theta(v_{r\theta}+v_{z\theta}v_{rz})\alpha_\theta + E_z(v_{rz}+v_{r\theta}v_{\theta z})\alpha_z]$$

$$\beta_\theta = \frac{1}{A} [E_\theta(v_{r\theta}+v_{z\theta}v_{rz})\alpha_r + E_\theta(1-v_{\theta z}v_{z\theta})\alpha_\theta + E_z(v_{rz}+v_{r\theta}v_{\theta z})\alpha_z]$$

$$\beta_z = \frac{1}{A} [E_\theta(v_{rz}+v_{r\theta}v_{\theta z})\alpha_r + E_z(v_{\theta z}+v_{\theta r}v_{rz})\alpha_\theta + E_z(1-v_{\theta z}v_{z\theta})\alpha_z]$$

Let the boundary surface of hollow cylinder be subject to time-dependent or constant boundary temperatures and pressures, the boundary conditions are

$$\sigma_r^*(r, z, t) = p(t) \quad , \quad \Theta_1 - \Theta_0 = f(t) \quad \text{at} \quad r^* = R_1$$

$$\sigma_r^*(r, z, t) = 0 \quad , \quad \Theta_2 - \Theta_0 = f_2 \quad \text{at} \quad r^* = R_0$$

$$\sigma_z^*(r, z, t) = 0 \quad , \quad \Theta_3 - \Theta_0 = f_3 \quad \text{at} \quad z^* = Z_0$$

$$\sigma_z^*(r, z, t) = 0 \quad , \quad \Theta_4 - \Theta_0 = f_4 \quad \text{at} \quad z^* = Z_1$$

At the interface between two adjacent layers, the following matching conditions must be satisfied:

$$U_j(r, t) = U_{j+1}(r, t) \quad r^* = R_j$$

$$\sigma_{r_j}^*(r, t) = \sigma_{r_{j+1}}^*(r, t) \quad r^* = R_j$$

$$q_j = q_{j+1} \quad r^* = R_j$$

$$\bar{\Theta}_j(r, t) = \bar{\Theta}_{j+1}(r, t) \quad r^* = R_j$$

$$i = 2, 3, \dots, m-1$$

The initial conditions are $U = \dot{U} = \bar{\Theta} = \dot{\bar{\Theta}} = 0$ at $t=0$

Substituting the non-dimensional quantities into the governing equations (1)-(3),

stress-displacement relations (4)-(7), we obtain the following nondimensional equations:

$$\left\{ a_k \frac{\partial^2}{\partial r^2} + \frac{b_k}{r} \frac{\partial}{\partial r} + c_k \frac{\partial^2}{\partial z^2} \right\} T = \frac{\partial T}{\partial r} + \frac{\partial}{\partial r} \left(\frac{\partial u_r}{\partial r} \right) + \frac{w_k}{r} \left(\frac{\partial u_r}{\partial r} \right) + x_k \frac{\partial}{\partial z} \left(\frac{\partial u_z}{\partial z} \right) \quad (8)$$

$$\frac{\partial^2 u_r}{\partial r^2} + \frac{1}{r} \frac{\partial u_r}{\partial r} - \frac{\phi_k}{r^2} u_r + d_k \frac{\partial^2 u_r}{\partial z^2} + e_k \frac{\partial^2 u_z}{\partial r \partial z} - f_k \frac{\partial T}{\partial r} - \frac{g_k}{r} T = 0 \quad (9)$$

$$\frac{\partial^2 u_z}{\partial r^2} + \frac{1}{r} \frac{\partial u_z}{\partial r} + h_k \frac{\partial^2 u_r}{\partial r \partial z} + i_k \frac{\partial^2 u_z}{\partial z^2} + h_k \frac{1}{r} \frac{\partial u_r}{\partial z} - j_k \frac{\partial T}{\partial z} = 0 \quad (10)$$

$$\sigma_{r,k} = Q_k \frac{\partial u_r}{\partial r} + {}_2Q_k \frac{u_r}{r} + {}_3Q_k \frac{\partial u_z}{\partial z} - {}_4Q_k T \quad (11)$$

$$\sigma_{\theta,k} = {}_1R_k \frac{\partial u_r}{\partial r} + {}_2R_k \frac{u_r}{r} + {}_3R_k \frac{\partial u_z}{\partial z} - {}_4R_k T \quad (12)$$

$$\sigma_{z,k} = P_k \frac{\partial u_r}{\partial r} + {}_2P_k \frac{u_r}{r} + {}_3P_k \frac{\partial u_z}{\partial z} - {}_4P_k T \quad (13)$$

$$\tau_{rz,k} = s_k \left[\frac{\partial u_z}{\partial r} + \frac{\partial u_r}{\partial z} \right] \quad (14)$$

The nondimensional boundary and interface conditions can be written as:

1. Boundary condition:

$$\sigma_r(r, z, t) = \frac{p(t)}{\beta_r \Theta_0} \quad , \quad T_i = f(t) / \Theta_0 \quad \text{at} \quad r = r_1$$

$$\sigma_r(r, z, t) = 0 \quad , \quad T_{out} = f_2 / \Theta_0 \quad \text{at} \quad r = r_0$$

$$\sigma_z(r, z, t) = 0 \quad , \quad T_{z1} = f_3 / \Theta_0 \quad \text{at} \quad z = z_1$$

$$\sigma_z(r, z, t) = 0 \quad , \quad T_{zout} = f_4 / \Theta_0 \quad \text{at} \quad z = z_0$$

2. Interface conditions:

$$u_i(r, z, t) = u_{i+1}(r, z, t) \quad r = r_{i+1}$$

$$\sigma_{ri}(r, z, t) = \sigma_{ri+1}(r, z, t) \quad r = r_{i+1}$$

$$q_i = q_{i+1} \quad r = r_{i+1}$$

$$T_i(r, z, t) = T_{i+1}(r, z, t) \quad r = r_{i+1}$$

$$i = 2, 3, \dots, m-1 \text{ layer}$$

Applying central difference scheme and Laplace transformation in equations (8)-(14), using boundary conditions into equations, we obtain the following equation in matrix form

$$\{[A] - s[I]\} \{T_{ij}\} + s[B] \{u_{r,ij}\} + s[C] \{u_{z,ij}\} - [Q] - [R] = [M] \quad (15)$$

$$[D] \{T_{ij}\} + [E] \{u_{r,ij}\} + [F] \{u_{z,ij}\} = 0 \quad (16)$$

$$[G] \{T_{ij}\} + [H] \{u_{r,ij}\} + [L] \{u_{z,ij}\} = 0 \quad (17)$$

Substituting equations (16) and (17) into equation (15), we have

$$\{[W] - s[I]\} \{\bar{Y}_{ij}\} = \{\bar{Y}_{ij}\} \quad (18)$$

where

$$[W] = \{ \{ [B]^{-1} [C] - [E]^{-1} [F] \} \{ [H] [E]^{-1} [F] - [L] \}^{-1} \{ [G] - [H] [E]^{-1} [D] \} + \{ [B]^{-1} + [E]^{-1} [D] \} \}^{-1} [B]^{-1} [A]$$

$$[\bar{Y}] = \{ \{ [B]^{-1} [C] - [E]^{-1} [F] \} \{ [H] [E]^{-1} [F] - [L] \}^{-1} \{ [G] - [H] [E]^{-1} [D] \} + \{ [B]^{-1} + [E]^{-1} [D] \} \}^{-1} [B]^{-1} \{ [M] + [Q] + [R] \}$$

The following solutions are obtained immediately from equation (18).

3. Numerical Results and Discussions

In this section, we present some numerical results of the temperature distribution in a finitely long hollow cylinder, and displacement and thermal stresses. To illustrate the foregoing analysis, we performed numerical calculations for multilayered hollow cylinder under an axisymmetric heating at the boundary surface. For a convenient solution to the example, consider in this paper, use isotropic material to analyze problems. For a finitely long hollow cylinder, the geometry and the material quantities of the cylinder are shown in Table 1. The diameter over length are assumed to be 3.2, respectively. The inner and outer temperatures are assumed to be $f(t)$ and 0 respectively. The inner and outer pressures are assumed to be $p(t)$ and 0 respectively. Temperatures at both ends are also assumed to

be 0 respectively. The both ends are traction free.

Figure 2 shows water vapor temperature and pressure relation assumed for the inner boundary. The water vapor temperature and pressure data were obtained from a thermodynamic steam table [6]. Figure 3 shows the temperature distributions with time. Figure 4 shows the pressure distributions with time. Figure 5 shows that the temperature distribution along radial direction and z-direction of multilayered hollow cylinder at $t=3$, respectively. The results show that when the temperature distribution in transient. Figure 6 shows the variation of radial displacement along radial and z directions for multilayered hollow cylinders at $t=3$, respectively. Figure 7 shows the z-direction displacement varying in r and z directions of multilayered hollow cylinder at $t=3$, respectively. The z-direction displacement changes with respect to time. Figure 8 shows the radial thermal stress distribution σ_r along the radial and z-directions at $t=3$, respectively. Figure 9 shows the circumferential stress σ_θ along radial and z-directions of multilayered hollow cylinder at $t=3$, respectively. Figure 10 shows that the stress distribution σ_z along radial and z-directions of multilayered hollow cylinder at $t=3$, respectively. Figure 11 shows that the distribution of shear stress τ_{rz} of hollow cylinders at $t=3$, respectively. The results show that this shear stress is very small as compared to other thermal stress components.

4. Conclusions

In this paper, we discussed completely the thermoelasticity problem of multilayered hollow cylinder whose boundaries are

subjected to time-dependent temperatures and pressures. The three-dimensional quasi-static axisymmetric coupled thermoelastic problem of multilayered hollow cylinder was discussed.

In the case of finitely long cylinder, numerical results of multilayered hollow cylinder at transient were calculated. The finite difference and Laplace transform methods were employed to obtain the numerical results. The temperature, displacement and thermal stress distributions were obtained which can be applied to mechanical part in precision measurement or design useful structures applications. The proposed method may be readily extended to solve a time wide range of physical engineering problems.

References

1. Stasyuk, S. T., Gromovik, V. I. and Bichuya, A. L., Thermal-Stress Analysis of Hollow Cylinder with Temperature-Dependent, Acad. of Sciences of the Ukrainian SSR, LVOV. USSR, Vol. 2, pp. 41-43, 1979
2. VoUbrecht, H., Stress in Cylindrical and Spherical Walls Subjected to Internal Pressure and Stationary Heat Flow, Verfahrenstechnik, Vol. 8, pp. 109-112, 1974
3. Kandil, A., Investigation of Stress Analysis in Compound Cylinders Under High Pressure and Temperature, M.Sc.Thesis, CIT Helwan, 1975.
4. Sinha, R. N., Thermal Stress Analysis of a Hollow Thick Cylinder by the Finite Element Method, J. Inst. Eng. (India) Mech. Eng. Division, Vol. 59, pp. 131-133, 1978
5. Naga, S. A. R., Optimum Working Conditions in Thick Walled Cylinders, J.

Eng. Mater. Technol. Trans. ASME, Vol. 108, pp. 374-376, 1986

6. Wylen G. V., Sanntag R, Borgnakke C., Fundamentals of Classical Thermodynamics, Fourth Edition, New York, 1994.

Nomenclature

r	non-dimensional radial coordinate
λ	Lame's constant
ρ	density
C_v	specific heat
Θ_0	reference temperature
L	z-direction length
$\nu_{\theta r}, \nu_{r\theta}$	Poisson's ratio
f_1, f_2	inner and outer surrounding temperatures
Θ, T	dimensional and non-dimensional temperature
U_r, u	dimensional and non-dimensional displacement
τ, t	dimensional and non-dimensional time
r^*, θ, z	cylindrical coordinate
k_r, k_θ, k_z	thermal conductivity
$\alpha_r, \alpha_\theta, \alpha_z$	linear thermal expansion coefficient
E_r, E_θ, E_z	Young's modulus
$\sigma_r^*, \sigma_\theta^*, \sigma_z^*$	dimensional stress
$\sigma_r, \sigma_\theta, \sigma_z$	non-dimensional stress

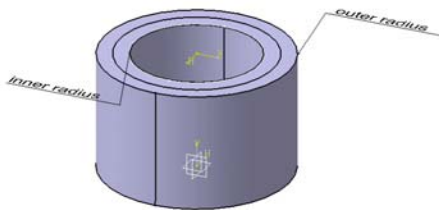


Figure 1. Physical model and system coordinates of multilayered hollow cylinder

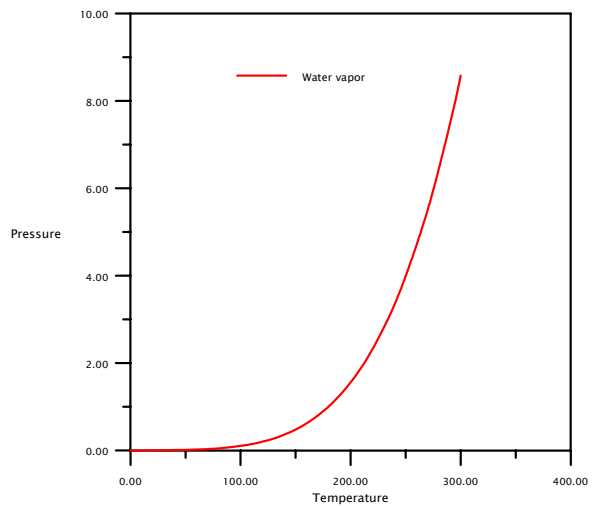
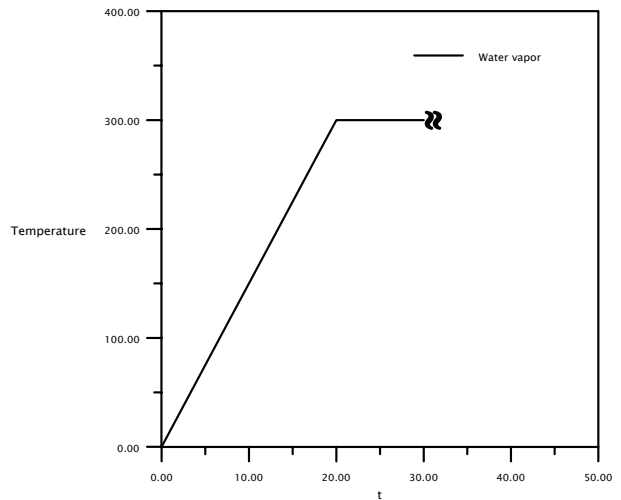
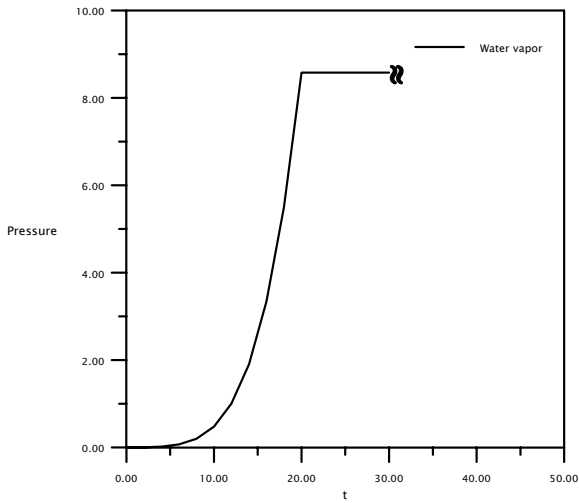


Figure 2. Temperature and pressure relation in inner boundary (quality 90%)[6]



$$f(t) = \begin{cases} 15t & , 0 \leq t \leq 20 \\ 300 & , t > 20 \end{cases}$$

Figure 3. Temperature distribution with time in inner boundary



$$p(t) = \begin{cases} -0.00013995t + 0.00461523t^2 - 0.00112473t^3 \\ + 0.00060406t^4 & , 0 \leq t \leq 20 \\ 8.585 & , t > 20 \end{cases}$$

Figure 4. Pressure distribution with time in inner boundary

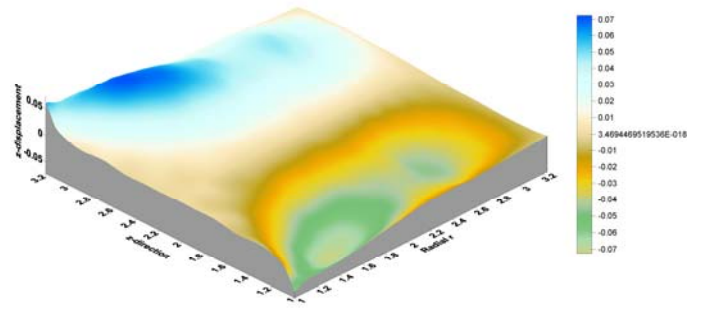


Figure 7. z-displacement along radial and z directions at t=3

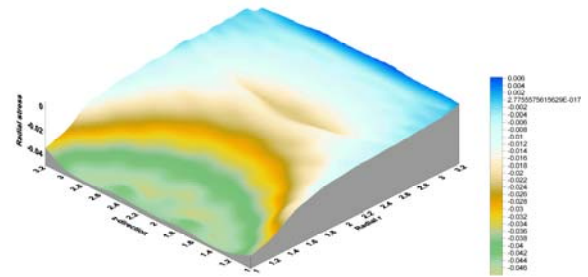


Figure 8. Radial stress along radial and z directions at t=3

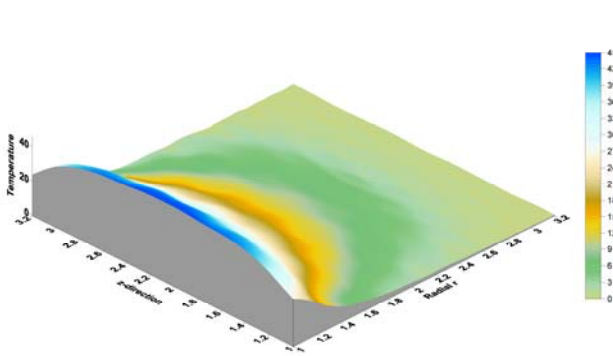


Figure 5. Temperature distribution along radial and z directions at t=3

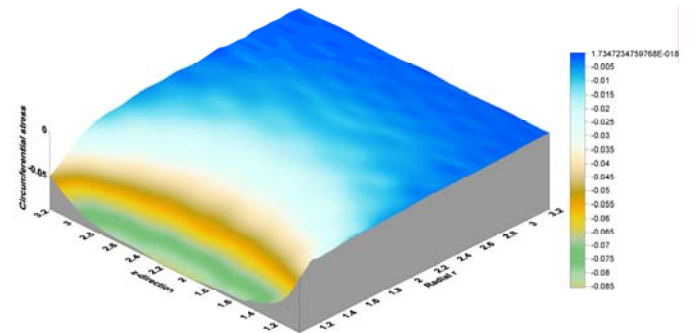


Figure 9. Circumferential stress along radial and z directions at t=3

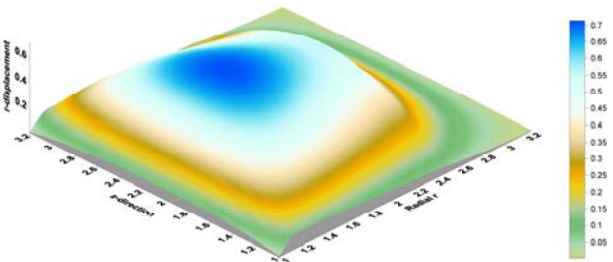


Figure 6. r-displacement along radial and z directions at t=3

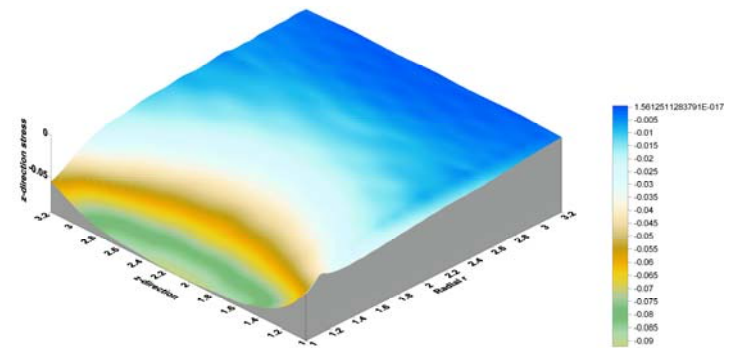


Figure 10. Stress distribution σ_z along radial and z directions at t=3

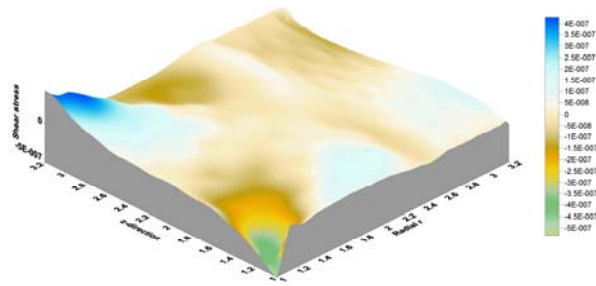


Figure 11. Shear stress distribution τ_{rz} along radial and z directions at $t=3$

Table 1.

The geometry and material constants of a finitely long hollow cylinder ($r_0/r_i = 3.2$, $z_0/z_1 = 3.2$)

	Layer 1	Layer 2
$E_r = E_\theta = E_z \left(\frac{N}{m^2} \right)$	58E6	50E6
$k_r = k_\theta = k_z \left(\frac{Watt}{m \cdot K} \right)$	22	10
$\alpha_r = \alpha_\theta = \alpha_z \left(\frac{1}{K} \right)$	4E-6	2E-6
$\nu_{r\theta} = \nu_{\theta r}$	0.2	0.4
$\nu_{rz} = \nu_{zr}$	0.2	0.4
$\nu_{z\theta} = \nu_{\theta z}$	0.2	0.4
$G_{zr} \left(\frac{N}{m^2} \right)$	58E6	50E6
$\rho \left(\frac{kg}{m^3} \right)$	0.095	0.085
$C_v \left(\frac{kJ}{kg \cdot K} \right)$	0.3	0.2